Ionosphere Effect Mitigation for Single-Frequency Precise Point Positioning

Constantin-Octavian Andrei, Ruizhi Chen, Heidi Kuusniemi, *Finnish Geodetic Institute, Finland*
Manuel Hernandez-Pajares, José Miguel Juan, Dagoberto Salazar, *Technical University of Catalonia (gAGE/UPC), Spain*

BIOGRAPHIES

Constantin-Octavian Andrei is a Senior Research Scientist at the Department of Navigation and Positioning at the Finnish Geodetic Institute. He received his diploma in Cadastral Surveying and Geodesy in 1999 from the Technical University of Iasi, Romania and a MSc degree in Geodesy and Geoinformatics in 2006 from the Royal Institute of Technology, Sweden. He is a PhD candidate at the Technical University of Iasi, Romania and at the Helsinki University of Technology, Finland. His research interests are satellite navigation and positioning techniques, satellite geodesy, theory of errors and network adjustment.

Dr. Ruizhi Chen is the Professor and Head of the Department of Navigation and Positioning at the Finnish Geodetic Institute. He holds a M.Sc. degree in computer science and a Ph.D degree in geodesy. His research interests include satellite-based augmentation systems, multi-sensor positioning, pedestrian navigation and mobile mapping systems.

Dr. Heidi Kuusniemi received her M.Sc. degree in 2002 and D.Sc. (Tech.) degree in 2005 from Tampere University of Technology, Finland. Her doctoral studies on personal navigation were partly conducted at the Department of Geomatics Engineering at the University of Calgary, Canada. After working as a GPS Software Engineer at Fastrax Ltd from 2005 to 2009, she joined the Department of Navigation and Positioning at the Finnish Geodetic Institute in May 2009 as a Specialist Research Scientist with research interests including various aspects of GNSS and sensor fusion.

Dr. Manuel Hernandez-Pajares is an associated professor of the Department of Applied Mathematics IV at the Polytechnical University of Catalonia (UPC) since 1993. He started working on GPS in 1989 for cartographic and surveying applications. Since 1995, his focus has been in the area of GNSS ionospheric determination and precise radionavigation. He was the Ionosphere WG chairman and Ionospheric product coordinator of the International GPS Service (IGS) from 2002 to 2009.

Dr. J. Miguel Juan Zornoza is an associate professor of the Department of Applied Physics at the Polytechnical University of Catalonia (UPC). His current research interest is in the area of GPS ionospheric tomography, GPS data processing algorithms, and radionavigation.

Dagoberto Salazar is an Aeronautical Engineer (IUPFAN, Venezuela, 1992). After working several years both for the government and in private industry, he pursued postgraduate studies in Instrumentation and Control (UCV). He is currently a PhD candidate in Aerospace Science and Technology at the Polytechnical University of Catalonia (UPC), as well as official developer of the GPS Toolkit project (GPSTk).

ABSTRACT

Precise Point Positioning (PPP) is a stand-alone positioning technique that has continuously increased the interest of the GNSS community in the last years, as the accuracy of the precise satellite orbit and clock data products has achieved centimeter-level. Combining these products with dual-frequency GNSS receiver data, the PPP approach is able to provide solutions at centimeter to decimeter level. Apart from the dual-frequency receiver users, there is a broad range of applications that use single-frequency-only receivers. For these users, the ionosphere represents the most critical source of error. This paper carries out an initial investigation on PPP performance using single-frequency code and carrier-phase data with different approaches to mitigate the ionospheric effect, such as the broadcast ionospheric model, Global Ionospheric Maps and Wide-Area Real Time Kinematic derived ionospheric corrections. An alternative way to remove the ionosphere influence is to take advantage of the fact that the group delay in the range observable and the carrier phase advance have the same magnitude but are opposite in sign. This paper also investigates the potential of this approach. Data retrieved from IGS stations covering different latitudes and solar activity periods (high, medium, low) are considered. The results show that sub-meter-level positioning accuracy can be obtained with single-frequency-only data utilizing proper ionospheric effect mitigation methods, under optimal multipath conditions. These initial results open the way to a broader study covering other single-frequency PPP ionospheric effect mitigation strategies, as well as harsher multipath conditions.

INTRODUCTION

Precise Point Positioning (PPP) has become more popular since the Selective Availability was turned off in May 2000. It has received increased interest from the GNSS community because of its flexibility, simplicity and cost-effectiveness (Gao and Shen, 2002). PPP determines a user position using the pseudorange and carrier phase observations from a single receiver in combination with precise satellite orbit and clock data products. In the last decade, it has been demonstrated that PPP is capable of providing accurate position solutions at centimeter level for static applications, and at decimeter level for kinematic applications, using a dual frequency receiver, (Zumberge et al., 1997; Heroux et. al, 2004; Gao et al., 2005).

However, a significant number of GNSS applications use single-frequency-only GNSS receivers. For this type of receivers, the ionospheric effect becomes the dominant source of error when the precise point positioning technique is used. As a result, it is important to investigate and evaluate various methods how to mitigate the ionospheric effect in single-frequency precise point positioning.

The simplest and the most popular method to mitigate the ionospheric error is the use of the ionospheric coefficients broadcast from GNSS satellites in combination with the Klobuchar model. Although this method has the advantage that it can be also implemented in real-time, the Klobuchar model with broadcast ionospheric coefficients can only mitigate 50-60% of the total ionospheric effect (Klobuchar, 1996).

The second method analyzed uses the Global Ionospheric Maps (GIMs) provided by the International GNSS Service (IGS) on a global scale since 1998. GIMs have a temporal resolution of 2 hours and a spatial resolution of 5 degrees (longitude) and 2.5 degrees (latitude). Currently, GIMs can provide an accuracy of 2 TECU (1 TECU corresponds to 0.163 m of range error in the C/A-code). However, the accuracy degrades for the interpolated points (Øvstendal, 2002). Comparing with the simple Klobuchar model, GIMs can provide better results, reducing approximately 75 to 80% of the ionospheric effect (Klobuchar and Kunches, 2000).

The third method assessed includes using the ionospheric correction data provided by an additional augmentation service such as the Wide-Area Real Time Kinematic (WARTK). Besides ionospheric corrections, WARTK also provides confidence values of the ionospheric corrections, DCBs and satellite clocks. This work will use a very simple approach to the WARTK technique, applying only the ionospheric corrections and DCBs instead of a full application of all the WARTK-provided parameters.

The last method assessed considers the single frequency ionospheric-free code and phase observable known as GRAPHIC – GRoup And PHase Ionospheric Combination (Yunck, 1996). Combining code and phase measurements has the advantage of a complete removal of the first-order ionospheric error. However, the phase ambiguity needs to be estimated. As a result, a long time period is required for the float ambiguities to stabilize and converge. In addition, the noise in this combination is dominated by the code measurement noise. Montenbruck (2003) demonstrated a 1.5 m 3D positioning accuracy in determining orbits of low Earth-orbit (LEO) satellites using C/A-code and L1 phase observations from non-geodetic space-borne GPS receivers.

The goal of this paper is to investigate the performance of all four ionospheric error mitigation methods for single-frequency PPP. The performance of the methods is evaluated based on the accuracy and precision of the derived solutions, as well as the post-fit measurement residuals. Numerical results demonstrate that GRAPHIC and WARTK methods can provide the best results with position accuracy from a few centimeters to decimeter-level. In addition, the GIMs and Klobuchar methods are able to provide point-positioning solutions better than 1 m for a session duration less than an hour, but depending on the ionospheric conditions.

IONOSPHERIC DELAY

The influence of the ionosphere on signal propagation in the radio frequency domain is mainly characterized by dispersion. The refraction coefficient describing the propagation of signal carrier phases can be written as a power series

$$(1) \quad n_{ph} = 1 + \frac{c_2}{f^2} + \frac{c_3}{f^3} + \frac{c_4}{f^4} + \dots$$

The coefficients c_i are independent of the carrier frequency f. However, they depend on the state of the ionosphere through the number of electrons per cubic meter (i.e., the electron density N_e) along the propagation path. Using an approximation by cutting off the series expansion, Eq. (1) becomes:

$$(2) \quad n_{ph} = 1 - \frac{40.3 N_e}{f^2}$$

with N_e representing the electron content along the signal propagation path, and f is the carrier frequency.

The ionospheric effect on code propagation (group delay) is, at first order, of the same size as the carrier phase propagation but with opposite sign:

$$(3) \quad n_{gr} = 1 + \frac{40.3 N_e}{f^2}$$

Integration over the entire propagation path, s, will yield the total effect of the ionospheric refraction on the pseudorange measurement ($dion_{gr}$):

$$(4)\quad dion_{gr} = \int (n_{gr} - 1) ds \approx \frac{40.3}{f^2} \int N_e ds$$

Defining the total electron content (TEC) by

$$(5)\quad TEC = \int N_e ds$$

and substituting the TEC into Eq. (4) yields

$$(6)\quad dion_{gr} = \frac{40.3}{f^2} TEC$$

It can be seen from Eqs. (2) and (3) that the group and phase refraction indices deviate from unity with opposite sign. As a consequence, the code measurements are delayed and the carrier phases are advanced. Introducing the notation

$$(7)\quad dion = \frac{40.3}{f^2} TEC$$

and omitting the subscripts "ph" and "gr", the ionospheric influence for the code pseudorange is modeled by $+dion$ while for the carrier phase by $-dion$.

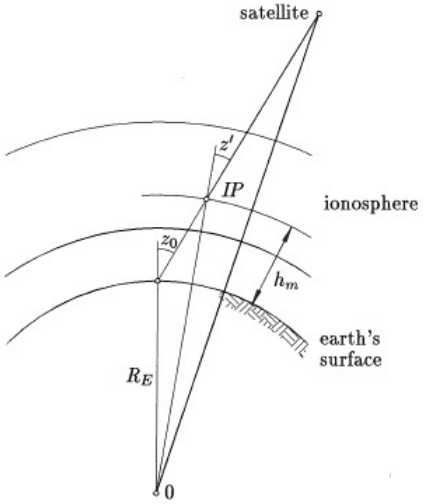

Figure 1: Single layer ionospheric model (Hofmann-Wellenhof et. al, 2008, p. 121)

Figure 1 illustrates a single-layer ionospheric model with the assumption that all free electrons are concentrated in a thin spherical shell at height h_m and containing the ionospheric point. For any arbitrary line of sight, the zenith angle of the satellite must be taken into account:

$$(8)\quad STEC = \frac{1}{\cos z'} VTEC$$

which leads to

$$(9)\quad dion = \frac{40.3}{f^2} STEC$$

with $STEC$ and $VTEC$ denoting the slant and zenith value of TEC, respectively. The zenith angle at the ionospheric point (IP) z' is obtained from

$$(10)\quad \sin z' = \frac{R_E}{R_E + h_m} \sin z_0$$

where R_E is the mean radius of the earth and z_0 is the zenith angle at the observing site. For h_m a value in the range of 300 –500 km is typical.

The resulting range error depends mainly on the solar activity, thus it varies with frequency, geographic location and time of day. For GPS frequencies, the error can vary from less than 1 m to more than 100 m (Wells, 1986; Klobuchar, 1996).

OBSERVATION EQUATIONS FOR SINGLE-FREQUENCY PRECISE POINT POSITIONING

The basic single-frequency code and phase observation equations can be written as:

$$(11)\quad \begin{aligned} P_i &= \rho + c(dt - dT) + dorb + drel + dtrop + dion_i \\ &\quad + b_{P_i} + b^{P_i} + det + dol + derp + dpcv + \varepsilon_{P_i} \end{aligned}$$

$$(12)\quad \begin{aligned} \Phi_i &= \rho + c(dt - dT) + dorb + drel + dtrop - dion_i \\ &\quad + \lambda_i (N_i + b_{\Phi_i} + b^{\Phi_i}) + det + dol + derp \\ &\quad + dpwu_i + dpcv + \varepsilon_{\Phi_i} \end{aligned}$$

where

i	identifies the frequency dependent terms
P_i	the code measurement (pseudorange) (m)
Φ_i	the carrier-phase measurement (m)
ρ	the geometrical range between satellite and GNSS receiver (m)
c	the vacuum speed of light (m/s)
dt	the receiver clock bias (s)
dT	the satellite clock bias (s)
$dorb$	the satellite orbit error (m)
$drel$	the relativistic delay (m)
$dtrop$	the tropospheric delay (m)
$dion_i$	the ionospheric delay (m)
λ_i	the wavelength of the carrier phase (m)
N_i	the integer carrier-phase ambiguity (cycles)
$dpwu_i$	the phase wind-up effect (m)
det	the solid earth tide effect (m)
dol	the ocean loading effect (m)
$derp$	the earth rotation parameters effect (m)
$dpcv$	the combined effect of the satellite antenna phase center variations and the receiver antenna phase center offsets (m)

b_{Φ_i} the receiver carrier-phase bias (cycles)

b^{Φ_i} the satellite carrier-phase bias (cycles)

b_{P_i} the receiver code bias (m)

b^{P_i} the satellite code bias (m)

$\varepsilon_{P_i}, \varepsilon_{\Phi_i}$ the measurement noise components, including multipath (m)

For precise point positioning, a number of additional modeling considerations must be taken into account that may not have been considered in pseudorange or even precise differential phase processing modes. These include the relativistic satellite clock correction ($drel$) due to the eccentricity in the satellite orbits; the satellite phase wind-up due to the relative rotation of the satellite antennas with respect to receiver antenna ($dpwu$); the phase-center variations of satellite and receiver antennas ($dpcv$); solid Earth tides (det), ocean tide loading (dol); sub-diurnal variations in Earth rotation ($derp$); and consistency between the models used to generate the precise satellite orbits and clocks and the models used in point positioning processing (Kouba and Héroux, 2002).

When the precise satellite orbit and clock products are used, the orbit error ($dorb$) and clock error (dT) can be neglected. For single-frequency users applying precise ephemerides and precise satellite clock information, which always refers to the ionosphere-free linear combination, also a set of differential code biases (DCBs) of the satellites should be considered to correct P1-code measurements accordingly (Schaer et. al., 1998). Alternatively, if clock corrections from broadcast ephemeris are used, the total group delay (T_{gd}) of a satellite should be taken into account. Additionally, DCBs between P1 and C1 (C/A-code) measurements, which are also satellite dependent, should also be applied (Jefferson et al., 2001). As to the receiver related DCBs between P1, P2 and C1, they are absorbed by the receiver clock parameters.

The tropospheric delay also can be corrected at centimeter level, using existing models and meteorological parameters. The tropospheric delay consists of two components: a hydrostatic component and a wet component. The hydrostatic zenith delay can be determined with an accuracy of 1.5-3 mm if pressure measurements are available. Conversely, the wet zenith delay is less predictable and, thus, it is considered as unknown parameter by the standard PPP algorithm in the estimation process. As a result of all these above-mentioned considerations, the observation equations (11) and (12) can be simplified to the following:

$$(13)\quad P_i = \rho_i + cdt + m_w zwd + dion_i + \varepsilon_{P_i}$$

$$(14)\quad \Phi_i = \rho_i + cdt + m_w zwd - dion_i + \lambda_i \overline{N}_i + \varepsilon_{\Phi_i}$$

with

m_w identifying the wet mapping factor

zwd the wet component of the tropospheric delay

and

$$(15)\quad \overline{N}_i = N_i + b_{\Phi_i} + b^{\Phi_i}$$

denoting the non-integer ambiguity of the carrier phase and ρ_i denoting the instantaneous range between the phase center of the satellite and receiver antenna including Earth tides, ocean loading, Earth rotation, and relativistic effects.

A Kalman filter procedure described in (Kalman, 1960) is applied to the observation equations for sequential estimation of four types of parameters: receiver position (dx, dy, dz), receiver clock (dt), tropospheric zenith wet delay (zwd), and carrier-phase ambiguities ($\overline{N}_i$).

As can be observed from Eqs. (13) and (14), the ionospheric effect becomes the major source of error in single-frequency PPP and it must be mitigated as precisely as possible. Several mitigation methods are discussed in the following section.

IONOSPHERE EFFECT MITIGATION

In this section four different methods for ionosphere effect mitigation are briefly described.

Method 1: Broadcast ionospheric model

The navigation message broadcast by the satellites contains a predicted ionospheric model (four α and four β parameters) that can be used with the Klobuchar model to correct single frequency observations (Klobuchar, 1996). During normal operation, the parameters of the model are updated at least once every six days (ARINC Engineering Services, 2004). The inputs in the Klobuchar model are the user geodetic latitude, the longitude, the time of day at the intersection between the mean ionospheric layer and the receiver to satellite line of sight, as well as the relative azimuth and elevation angle of the satellite (see Figure 1). This model can provide a correction for about 50% root-mean-square (RMS) of the ionospheric range delay (Klobuchar, 2000).

Since mid of July 2000, the Center for Orbit Determination in Europe (CODE) has been providing on a regular basis Klobuchar-style ionospheric coefficients (alphas and betas) best fitting its global ionosphere maps. A validation study based on two months of data confirmed that the predicted coefficients perform significantly better than the coefficients broadcast by the GPS system for a single-frequency user (Schaer, 2001). In addition, coefficients derived from CODE final and rapid IONEX data, as well as coefficients based on 1-day and 2-day IONEX predictions are generated and provided. They are made available in form of content-reduced

RINEX navigation data files. Furthermore, the CODE analysis center is able to supply post-processing users of GPS broadcast ionospheric model with a unique, continuous time series of RINEX files containing improved Klobuchar-style ionospheric coefficients starting from January 1, 1995 (Schaer, 2001).

In this research, the CODE Klobuchar-style ionospheric coefficients were used together with the Klobuchar model.

Method 2: Global Ionospheric Maps

The IGS (International GNSS Service) ionosphere working group (Iono-WG) was established in May 1998, to produce ionospheric vertical total electron content (VTEC) maps as one of the IGS products for the GNSS community. Currently, four IGS Ionosphere Associate Analysis Centers (IAACs) operated by different agencies provide their ionosphere products as two-dimensional Global Ionosphere Maps (GIMs) in IONopshere Map Exchange (IONEX) format (Schaer et. al., 1998). Each IAAC generates its daily IONEX file that has 13 GIMs at 2-h intervals. These files are contributed to the Iono-WG in order to generate the combined IGS final and rapid product. Since April 2003, the final IGS GIMs in IONEX format have become an official IGS product, which are uploaded with a delay of about 11 days for public downloading. Meanwhile, a rapid version of GIMs is available to the public since December 2003 with a latency less than 24 hours. Both final and rapid IGS GIMs have a temporal resolution of 2 hours and a spatial resolution of 2.5 degrees north-south (latitude) and 5 degrees east-west (longitude). The accuracy varies from the level of 2 TEC (1 TECU corresponds to 0.163 m range error on L1 frequency) to about 8-9 TECU (IGS, 2009). The accuracy degrades for the interpolated points (Øvstendal, 2002).

When computing ionospheric corrections from the model, the inputs are the *geocentric* latitude and longitude of the ionospheric point. For this position, one computes the VTEC values at the observation epoch. In the temporal interpolation, the TEC maps are rotated around the Z-axis in order to compensate to a great extent the strong correlation between the ionosphere and the Sun's position. After that, interpolation between *consecutive rotated* TEC maps can be performed. In addition, for spatial interpolation, one may use a simple 4-point formula (bivariate interpolation), if the IONEX grid is dense enough (Schaer et. al., 1998). Finally, the interpolated VTEC values are then converted into slant TEC using Eq. (8) and into metric slant corrections using Eq. (9). Please also notice that GIMs always refer to a standard altitude of 450 km for the ionospheric layer (see Figure 1).

In this research, the combined IGS final ionospheric products were used to exploit the potential of the IGS ionospheric products.

Method 3: Wide-Area Real Time Kinematic derived ionospheric corrections.

The Wide-Area Real Time Kinematic (WARTK) is a very precise differential technique to compute ionospheric corrections in real-time using a 3-D voxel model of the ionosphere, estimated by means of a Kalman filter, and using exclusively GNSS data gathered from fixed receivers separated several hundreds of kilometers (Hernandez-Pajares 1999, 2000).

WARTK ionospheric corrections provided by gAGE/UPC co-authors were applied to the data, when available. In this work a simple approach was followed, taking advantage only of the ionospheric corrections and DCBs. Other WARTK products such as ionospheric corrections confidence values and satellite clocks were not used, impairing the full potential of this technique. Besides, given that WARTK is a differential technique, the performance degrades with distance from the nearest reference station.

This approach to the WARTK technique denoted henceforward as 'simplified WARTK' will set a worst-case scenario for its use in the single-frequency PPP strategy. Future work will be done to implement the full potential of this technique.

Method 4: GRAPHIC combination

The ionosphere-free code and phase combination (G_i) is the average of the code and phase measurement as follows:

$$G_i = \frac{P_i + \Phi_i}{2} = \rho_i + cdt + m_w ZWD + \frac{\lambda_i \overline{N}_i}{2} + \frac{\varepsilon_{P_i} + \varepsilon_{\Phi_i}}{2} \quad (16)$$

This combination is known also as GRAPHIC – GRoup And PHase Ionospheric Combination (Yunck, 1996). It is of particular interest in single-frequency space applications because it is able to eliminate all the ionospheric effect, but at the cost of having an ambiguity (from the carrier-phase measurement) and more noise than the pure carrier-phase combination. Most of the noise in this combination is due to C/A (P) code measurement error, while the noise and multipath of L_i is negligible with respect to the code. According to Yunck (1996), modern, high quality receivers in optimal low multipath environments can recover code pseudorange with a precision better than 50 cm in 1 s. The GRAPHIC observable reduces this by half.

With this method, the position coordinates and ambiguity parameters cannot be estimated using a single epoch of observations. Based on cumulative measurements, Heroux et al. (2004) found that the estimation process requires several hours for the float ambiguity to converge.

Within this study, the GRAPHIC method combines the ionosphere-free code and phase observation with ionospherically corrected code pseudorange observation.

NUMERICAL RESULTS AND ANALYSIS

In order to investigate the performance in ionosphere delay mitigation of the above-described methods, three different time intervals covering different solar activity periods (high, medium and low) were considered in the analysis (Table 1). For these time intervals, the corresponding IGS products, such as final precise satellite orbits and clock corrections, earth rotation parameters, and the combined final global ionospheric maps were used in the investigations. A cut-off elevation angle of 10º was applied to all datasets. The time interval of the collected data was 30 seconds. However, the data were decimated to 5 min to be consistent with the frequency of the WARTK ionospheric corrections.

Table 1: The geomagnetic (Ap) indices for three testing weeks covering different solar activity conditions.

Year	2002 (high solar activity)						
DoY	140	141	142	143	144	145	
Ap	10	10	8	78	2	4	
Year	2004 (medium solar activity)						
DoY	231	232	233	234	235	236	237
Ap	8	4	15	16	12	5	3
Year	2006 (low solar activity)						
DoY	345	346	347	348	349	350	351
Ap	14	27	8	47	94	12	6

An important rule in single-frequency PPP is to set realistic a priori code and carrier phase sigma values, which should reflect the actual uncertainty of these measurements. In fact the values themselves are not of great importance; only the fact that the variance of the code should be much greater than the variance of the phase measurement is significant for the final solution. This assumption was considered for three of the methods (Klobuchar, GIMs and WARTK). As for the GRAPHIC method, the model must take into account the fact that the noise of the GRAPHIC combination is 50% of the noise of the code measurement. Additionally, the code measurement variance has to be chosen taking into account the fact that the code measurement still contains the ionosphere influence. To reduce this influence, the GRAPHIC method combines the ionosphere-free code and phase observation with the ionospherically corrected pseudorange, using GIMs. Table 2 summarizes measurement variances (i.e., standard deviations squared) used in this paper.

The position solutions were generated using the Kalman filter formulation for static positioning considering Eqs. (13), (14) and (16).

Table 2: Measurement standard deviations considered by different mitigation methods. In addition, an elevation-dependent weighting approach was considered.

Method	Measurement standard deviations (m)	
	Code	Phase
Klobuchar	1.0	0.01
GIMs	1.0	0.01
WARTK	1.0	0.01
GRAPHIC	1.0	0.10

The estimated parameters were receiver position (three components), receiver clock, troposphere zenith wet delay, and carrier phase ambiguities (one for each satellite in view). The receiver position was treated as constant (i.e., static mode). The receiver clock drifts according to stability of its oscillator, e.g. several cms/seconds. Conversely, the troposphere zenith wet delay varies in time by a relatively small amount, in the order of a few cms/hour. The ambiguities remained constant as long as no cycle-slips occurred.

The obtained solutions were compared to the final IGS coordinates that were considered as true values in this article. The latitude, longitude, and height differences were transformed to a local topocentric coordinate system (NEU). The changes in topocentric coordinates were used to evaluate the accuracy of the results.

Static positioning in Catalonia, Spain

The positioning results presented in this section are obtained at two mid-latitude stations (EBRE and LLIV) operated by the Institute Cartografic de Catalunya (ICC), Spain. They are equipped with a TRIMBLE 4000SSI (until October 2005) and TRIMBLE NETRS (after October 2005) GPS receivers, and a TRM29659.00 antennas type.

Figure 2 and Figure 3 illustrate the accuracy statistics (3D RMS) using all the mitigation methods described before and arranged according with the day-of-year (DoY). From the figures, one can see that the GRAPHIC method provides the best accuracy with values around 10-15 cm for all the testing days regardless of the intensity of the solar activity.

The good results are explained by the fact that the chosen stations belong to IGS, implying the use of high quality receivers and antennas, with data collected in low multipath environments. This boosts the GRAPHIC combination performance because the IGS site conditions greatly reduce the combination noise.

For instance, Figure 4 shows the multipath effect in P1 for several stations. Stations BRUS, COCO, EBRE and ONSA belong to the IGS network, and show low multipath levels that are just a few times worse than the ionosphere-corrected L1 observable (whose sigma is also shown).

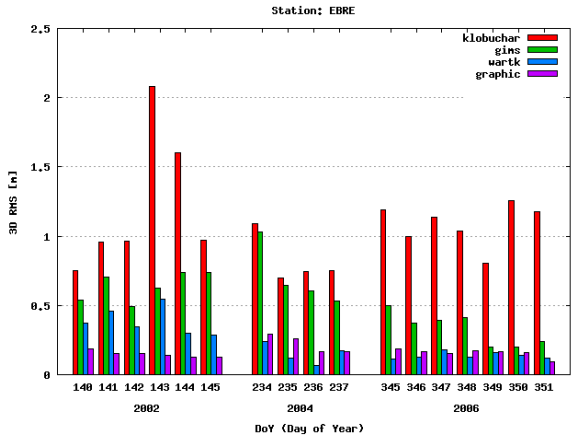

Figure 2: Positioning errors of different ionospheric error mitigation methods at EBRE under different periods of solar activity. From left to right: Klobuchar (*red*), GIMs (*green*), WARTK (*blue*), GRAPHIC (*magenta*). There is no GPS data for DoY 231-233.

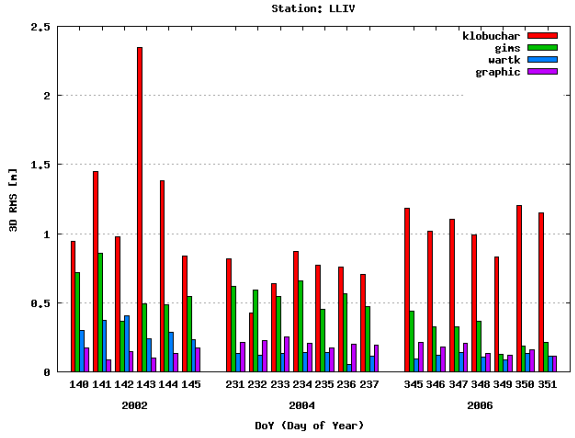

Figure 3: Positioning errors of different ionospheric error mitigation methods at LLIV under different periods of solar activity. From left to right: Klobuchar (*red*), GIMs (*green*), WARTK (*blue*), GRAPHIC (*magenta*).

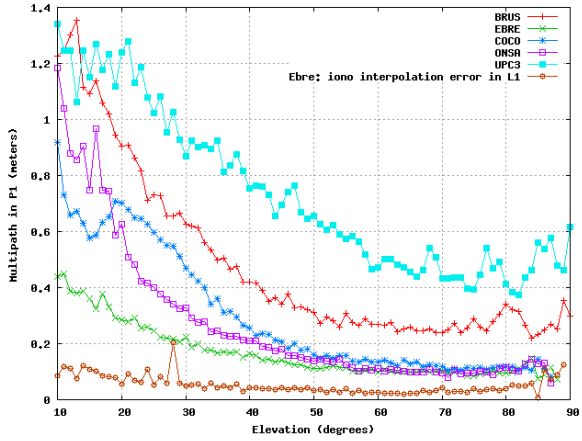

Figure 4: Multipath in P1 for IGS stations BRUS, EBRE, COCO and ONSA, plus non-IGS station UPC3.

The former low multipath levels are not realistic for single-frequency PPP scenarios. For example, UPC3 station combines a high quality receiver with a medium quality antenna, in a low to medium multipath environment, and shows about three times more multipath noise than EBRE. The expected multipath for a typical one-frequency PPP scenario (medium-to-low quality receivers and antennas) should be even worse.

The simplified WARTK method is able to offer accuracies close to the GRAPHIC method, although the accuracy decreases to half-meter for some testing days. The reason for that is weak satellite geometry (Figure 5) as not all the satellites in view have WARTK ionospheric corrections for the processed epoch. As a result, the Kalman filter algorithm removes these satellites from the solution computation at that specific epoch. A weak satellite geometry leads to a poor accuracy, especially, in the vertical (Up) component of the 3D error (Figure 6).

Another reason for the diminished WARTK performance is the non-standard use of the technique, where fixed values for variances are used instead of the WARTK-provided ionospheric sigmas.

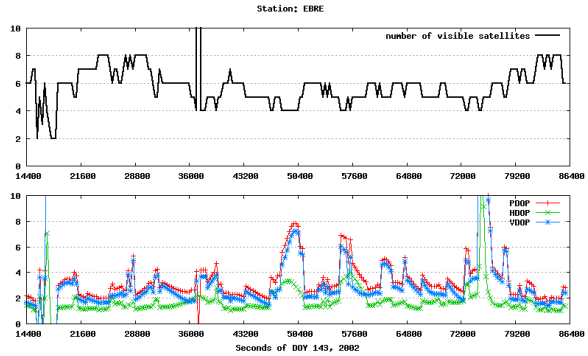

Figure 5: The PDOP number and the number of valid satellites with ionospheric corrections for the WARTK method at station EBRE for DoY 143, 2002.

Compared to the GRAPHIC and WARTK methods, the Klobuchar method performs much worse; only 1 to 2 meter accuracy was obtained. For all testing days, the Klobuchar method gives the less accurate results. The worst day is DoY 143, 2002 when the accuracy exceeds two meters. The result is related to ionospheric conditions for that day, with an Ap index of 78 in that day (Table 1). The Klobuchar model only uses eight coefficients to describe the ionosphere activity on a global scale and the coefficients may not perform well for some regions.

The GIMs method shows better results than Klobuchar at both stations for all days. For quite many days the accuracy for GIMs is almost twice larger than that obtained with WARTK or GRAPHIC. The GIMs performance depends on the station location inside the IGS tracking network, which is used to generate the ionospheric maps. As the station density is higher in the

mid-latitude region than the equatorial or high-latitude regions, it is expected that a weaker performance of this method is obtained for those regions.

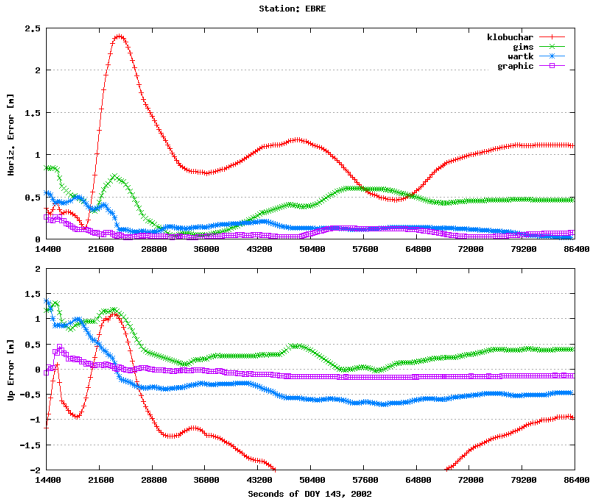

Figure 6: The horizontal and vertical component of the 3D error at EBRE for DoY 143, 2002 for different ionospheric error mitigation methods during active ionospheric conditions.

Positioning results at equatorial and high-latitude stations

To verify the performance of the mitigation methods, three of the methods (excluding WARTK) were also tested for two other stations considered representative for equatorial and high-latitude regions, respectively. While one station (COCO) is located in the southern hemisphere and belongs to the Australian Regional GPS Network (ARGN), the other one (ONSA) belongs to the Swedish network of permanent GPS reference stations (SWEPOS) and located at high-latitude. Their receiver and antenna types are shown in Table 3.

Table 3: IGS GPS receiver and antenna types

Station	Receiver type	Antenna Type
COCO	ASHTECH UZ-12	AOAD/M_T
ONSA	ASHTECH Z-II3	AOAD/M_B
	JPS E_GGD	

The accuracy statistics (3D RMS) of the positioning results for COCO station are presented in Figure 7, while the results for ONSA station are showed in Figure 8. The GRAPHIC method shows the same performance as for the mid-latitude stations. The method is almost insensitive to both the station location and the ionospheric conditions. In contrast, the positioning results obtained with GIMs and especially with Klobuchar approach show different performance. While for the high-latitude region the performance of the GIMs and Klobuchar is close to the performance as in the mid-latitude region, for the equatorial region the performance of the two methods is much worse. In addition, the performance is correlated to the ionospheric conditions; higher ionospheric activity leads to less accurate positioning solutions.

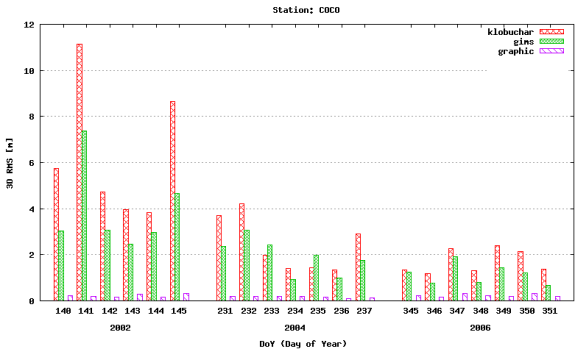

Figure 7: Positioning 3D error at COCO for three ionospheric effect mitigation methods.

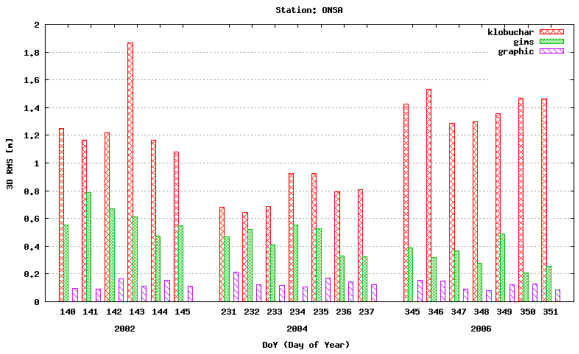

Figure 8: Positioning 3D error at ONSA for three ionospheric effect mitigation methods.

Measurement residual analysis

In order to investigate further the performance of the methods for ionosphere effect mitigation, this section presents the results of the analysis done in the residual domain, i.e., measurement residuals.

As expected, the residuals for the code measurements for the Klobuchar method show the highest values as the code measurement still contain almost half of the ionosphere influence. The results emphasize two main things: the intensity of the solar activity decreases from 2002 to 2006 and the ionospheric activity decreases from the equatorial regions to the high-latitude regions. The Klobuchar and GIMs code residuals are correlated with the ionospheric activity and their magnitude is influenced by the mismodeling errors. The best results are shown by the WARTK method.

On the other hand, the residuals for the phase measurement show much better accuracy with WARTK method being the best. The GRAPHIC method also shows results very similar to WARTK, with accuracies less than

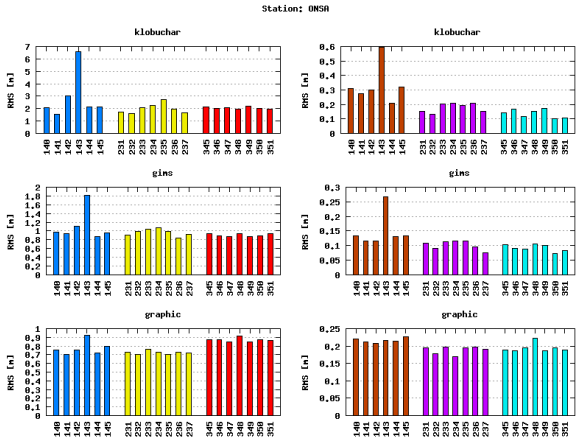

Figure 9: The code (*left*) and phase (*right*) measurement residual statistics (3D RMS) for ONSA.

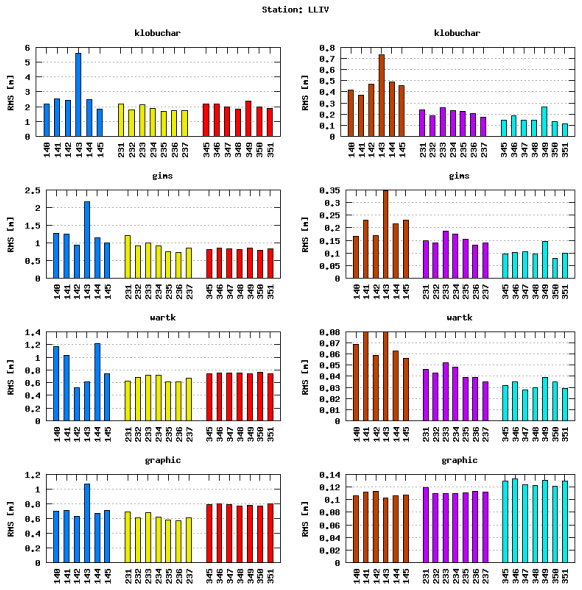

Figure 10: The code (*left*) and phase (*right*) measurement residual statistics (3D RMS) for LLIV.

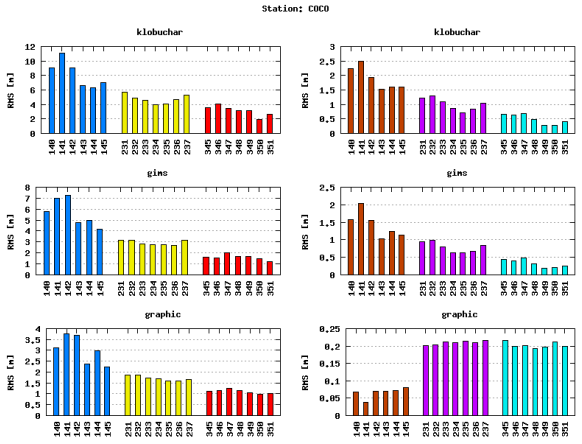

Figure 11: The code (*left*) and phase (*right*) measurement residual statistics (3D RMS) for COCO.

20 cm (around one cycle on L1, with low multipath environment). However, similar to code residuals, the Klobuchar and the GIMs phase residuals are dependent on the station location and the ionospheric conditions.

CONCLUSIONS AND FUTURE WORK

Different ionospheric error mitigation methods have been compared in this article for single-frequency precise point positioning. Except for the GRAPHIC method, the performance of all the other mitigation methods depends on the ionospheric conditions and station location. The position accuracy is higher during calm ionospheric days than on the days with increased ionospheric activity. Additionally, the position accuracy is better at mid-latitude and high-latitude stations than at the equatorial stations.

In general, the GRAPHIC method provides the best results among all the investigated methods for the low multipath scenarios of this work. The position solutions are stable and do not depend on the ionospheric conditions. However, this method requires some period of time for the ambiguity to converge. Although it is recommended to fix the ambiguities, float ambiguities are just enough for navigation and non high-accuracy applications.

The applied simplified WARTK method can provide position solutions with accuracy similar to the GRAPHIC method and with the best accuracy for the code and phase residuals. In addition, this method can be implemented for real-time applications and its performance may be greatly increased if applied in the standard way, i.e., taking also into account other WARTK products like ionospheric estimation variances and satellite clocks.

In the future, the research for single-frequency PPP will be continued, and related precise ionosphere modeling and estimation methods will be implemented and investigated. Further tests with kinematic data sets will also be considered, as well as full WARTK method implementation and medium-to-high multipah scenarios.

ACKNOWLEDGMENTS

The first author would like to thank the Finnish Geodetic Institute for the financial and technical supports offered in pursuing his doctoral research in Finland. The IGS data and combined solution products (Dow et al., 2005) used in the analysis presented are acknowledged. The authors would also like to acknowledge support from the GPSTk open source project (Tolman et al., 2004).

REFERENCES

[1] Gao, Y. and X. Shen (2002). *A New Method for Carrier Phase Based Precise Point Positioning.*

NAVIGATION, Journal of the Institute of Navigation, 49(2), 109-116.

[2] Zumberge, J.F., M.B Heflin, D.C. Jefferson, M.M. Watkins and F.H. Webb (1997). *Precise point positioning for the efficient and robust analysis of GPS data from large networks*, Journal of Geophysical Research, 102(B3), 5005–5017.

[3] Héroux, P., Y. Gao, J. Kouba, F. Lahaye, Y. Mireault, P. Collins, K. Macleod, P. Tétreault, and K. Chen (2004). *Products and Applications for Precise Point Positioning - Moving Towards Real-Time*. Proceedings of the 17th International Technical Meeting of the Satellite Division of the Institute of Navigation ION GNSS 2004, Long Beach, CA, September 21-24, 2004, 1832-1843.

[4] Gao, Y., A. Wojciechowski and K. Chen (2005). *Airborne Kinematic Positioning Using Precise Point Positioning Methodology*. Geomatica, 59(1), 29-36.

[5] Klobuchar, J.A. (1996). *Ionospheric Effects on GPS*, In: Parkinson, B.W. and J.J. Spilker Jr. (eds), Global Positioning System: Theory and Applications Volume I, Progress in Astronautics and Aeronautics, American Institute of Aeronautics and Astronautics, 163, Washington, D.C., 1996, 485-515.

[6] Øvstendal, O. (2002). *Absolute Positioning with Single-Frequency GPS Receivers*. GPS Solutions, 5(4), 33-44.

[7] Klobuchar, J.A. (2000). *Eye on the Ionoosphere: Correcting for Ionospheric Range Delay on GPS – Temporal Decorrelation*. GPS Solutions, 4(2), 78-82.

[8] Hernandez-Pajares, M., J.M. Juan, J. Sanz and O.L. Colombo. (1999). *Precise ionospheric determination and its application to real-time GPS ambiguity resolution*. Proceedings of ION GPS'99. Institute of Navigation. Nashville, Tennessee, USA, September 1999.

[9] Hernandez-Pajares, M., J.M. Juan, J. Sanz and O.L. Colombo. (2000). *Application of ionospheric tomography to real-time GPS carrier-phase ambiguities resolution, at scales of 400-1000 km, and with high geomagnetic activity.* Geophysical Research Letters, 27, 2009-2012. 2000.

[10] Yunck, T.P. (1996). *Orbit determination*, In: Parkinson, B.W. and J.J. Spilker Jr. (eds), Global Positioning System: Theory and Applications Volume II, Progress in Astronautics and Aeronautics, American Institute of Aeronautics and Astronautics, 164, Washington, D.C., 1996, Chapter 21, 559-591.

[11] Montenbruck, O. (2003). *Kinematic GPS positioning of LEO satellites Using Ionosphere-Free Single Frequency Measurements*. Aerospace Science and Technology, 7(5), 396-405.

[12] Wells, D.E., N. Beck, D. Delikaraoglou, A. Kleusberg, E.J. Krakiwsky, G. LaChapelle, R.B. Langley, M. Nakiboglu, K.P. Schwarz, J.M. Tranquilla, and P. Vanicek (1986). *Guide to GPS Positioning*. Canadian GPS Associates, Fredericton, New Brunswick, Canada, 291 pp.

[13] Schaer, S., W. Guntner and J. Feltens (1998). IONEX: *The IONosphere Map Exchange Format Version 1*, Proceedings of the IGS AC Workshop, Darmstadt, Germany, February 9-11, 1998, ESA/ESOC, 233-237.

[14] Kouba, J. and P. Héroux (2002). *Precise Point Positioning Using IGS Orbit and clock Products*. GPS Solutions, 5(2), 12-28.

[15] Jefferson, D., M.B. Heflin, and R.J. Muellerschoen, (2001). *Examining the C1-P1 Pseudorange Bias*. GPS Solutions, 4(4), 25-30.

[16] Kalman, R.E., (1960). *A New Approach to Linear Filtering and Prediction Problems*, Transaction of the ASME, Journal of Basic Engineering, 33-45, March 1960.

[17] ARINC Engineering Services (2004). *GPS Interface Specification IS-GPS-200, revision D: Navstar GPS Space Segment/Navigation User Interfaces*. CA, USA, 193 pp.

[18] Schaer, S. (2001). *Generating Klobuchar-Style Ionospheric Coefficients for Single-Frequency Real-Time and Post-Processing Users*, Printing Office, Astronomical Institute, University of Berne, August 21, 2001.

[19] IGS (2009). *International GNSS Service* <http://igscb.jpl.nasa.gov/> (May 2009).

[20] Dow, J.M., R.E. Neilan, and G. Gendt (2005). The International GPS Service: *Celebrating the 10th anniversary and looking to the next decade*. Advances in Space Research, 36(3), 320-326.

[21] Tolman, B., R.B. Harris, T. Gaussian, D. Munton, J. Little, R. Mach, S. Nelsen, and B. Renfro (2004). *The GPS Toolkit: Open Source GPS Software*. Proceedings of the 17th International Technical Meeting of the Satellite Division of the Institute of Navigation ION GNSS 2004, Long Beach, CA, September 21-24, 2004, 2044-2053.